Inorganic Chemistry

Article

pubs.acs.org/IC

Co_5/Co_8–Cluster-Based Coordination Polymers Showing High-Connected Self-Penetrating Networks: Syntheses, Crystal Structures, and Magnetic Properties

Dong-Sheng Li,*[,†,‡] Jun Zhao,[†] Ya-Pan Wu,[†] Bin Liu,*[,§] Liang Bai,[†] Kun Zou,[†] and Miao Du*[,∇]

[†]College of Mechanical & Material Engineering, Research Institute of Materials, China Three Gorges University, Yichang 443002, People's Republic of China

[‡]State Key Laboratory of Coordination Chemistry, Nanjing University, Nanjing 210093, People's Republic of China

[§]Department of Chemistry, Northwest University, Xi'an 710069, People's Republic of China

[∇]College of Chemistry, Tianjin Key Laboratory of Structure and Performance for Functional Molecules, MOE Key Laboratory of Inorganic–Organic Hybrid Functional Material Chemistry, Tianjin Normal University, Tianjin 300387, People's Republic of China

Supporting Information

ABSTRACT: Two novel Co(II)-cluster-based coordination polymers—namely, $[Co_5(\mu_3{-}OH)_2(1,4\text{-ndc})_4(bix)_2]_n$ (**1**) and $\{[Co_8(\mu_3{-}OH)_4(1,4\text{-ndc})_6(btp)(H_2O)_6]\cdot H_2O\}_n$ (**2**)—were prepared by hydrothermal reactions of Co(II) perchlorate with 1,4-naphthalenedicarboxylic acid (1,4-H_2ndc) and different N-donor coligands (bix = 1,4-bis(imidazol-1-ylmethyl)-benzene and btp = 4,4′-bis(triazol-1-ylmethyl)biphenyl). In **1**, 10-connected $[Co_5(\mu_3{-}OH)_2(COO)_8]$ clusters are extended by the μ_4-1,4-ndc^{2-} and *trans*-bix ligands to construct a rare, self-penetrating **ile** framework that can interestingly be regarded as the cross-link of two interpenetrating 6-connected **pcu** networks. While for **2**, $[Co_8(\mu_3{-}OH)_4(COO)_{12}]$ clusters serve as the 8-connected nodes, which are bridged by the μ_4/μ_5-1,4-ndc^{2-} and *trans*-btp ligands to afford the highest-connected uninodal self-penetrating ($4^{20}.6^8$) network based on octacobalt clusters. A synthetic and structural comparison of **1** and **2** demonstrates that the features of auxiliary N-donor ligands play a key role in governing the in situ formed clusters and the final 3-D coordination frameworks. Magnetic susceptibility measurements indicate that complex **1** shows an antiferromagnetic interaction between the adjacent Co(II) ions, whereas **2** displays the dominant antiferromagnetic exchanges in 300–50 K and a ferrimagnetic-like behavior at lower temperatures.

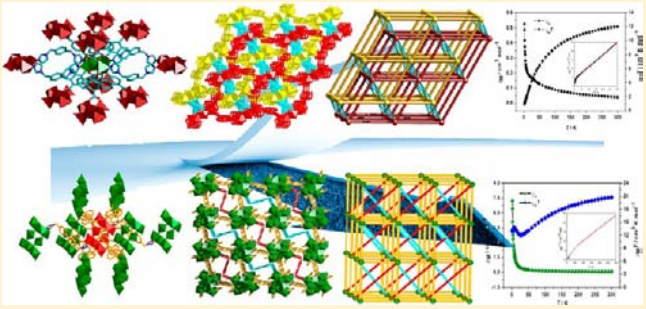

INTRODUCTION

The field of metal–organic frameworks (MOFs) or coordination polymers has continuously evolved since Hoskins and Robson first combined the inorganic and organic molecular units to create infinite networks in the early 1990s.[1] In fact, the driving force for this is that there exist endless possibilities and inexhaustible synthetic options to tailor their structures and properties, which provides a huge source of experimental systems for both fundamental science and potential applications.[2] As a result, in the realm of coordination polymers, many intriguing topological types and associated interesting properties have been investigated in-depth.[2,3] However, from the perspective of developing advanced crystalline materials, one of the most attractive targets is to establish a clear relationship between the network structures and properties of coordination polymers, which represents a great challenge, both experimentally and theoretically.

In this context, metal cluster-based MOFs have drawn particular attention, providing substantial impetus for the development of new materials with unique frameworks and properties, such as magnetism, gas adsorption/storage, catalysis, and luminescence.[4,5] Comparing with common approach using designed linkers and preselected metal centers as nodes for the rationalization of network topology, the construction of cluster-based MOFs with metal clusters as secondary building blocks (SBUs), is a rather complex process, because these SBUs are often generated in situ in different reactions.[6] Thus, the variable factors in the assembled processes will make significant structural changes of the resulting clusters. Besides, the current studies on cluster-based MOFs have shown that the organic linkers is crucial to govern the nuclearity and arrangement of metal ions,[7] in which the most well-known linkers are conjugate polycarboxylic acids that can bind several metal centers with specific coordination geometry to construct polynuclear clusters, such as $[Cu_2(OH)_2(COO)_4]$, $[Cr_3O(OH)_3(COO)_6]$, $[Co_4(OH)_2(COO)_6]$, and $[Zn_4O(COO)_6]$, etc.[8] Notably, in the polycarboxylato-metal clusters systems, the auxiliary N-

Received: March 28, 2013
Published: July 2, 2013

   dx.doi.org/10.1021/ic4007718 | *Inorg. Chem.* 2013, 52, 8091–8098

donor co-ligands can also induce their structural changes to result in distinct properties.

On the other hand, in cluster-based MOFs, the coexistence of water, hydroxide, and carboxylate has commonly been found to connect the metal ions to afford clusters, especially for Co(II) systems. Thus, the assemblies of Co(II) with multicarboxylates are apt to form various clusters,[9] such as Co_2, Co_3, Co_4, Co_5, Co_6, Co_7, Co_8, and Co_{12}, as well as chain/ladder/layer as the SBUs of MOFs.[9a,b] Recently, unusual 8-, 9-, 10-, and 12-connected MOFs based on Cd_3, Zn_5, Cd_5, and Co_4 clusters,[10] have been constructed from the mixed-ligand system of aromatic dicarboxylic acids and N-donor co-ligands, which also show interesting magnetic and luminescent properties.[10] Inspired by these results, we have continued the efforts on Co(II)-cluster based MOFs,[11] and herein chose the aromatic dicarboxyl tecton, 1,4-naphthalene dicarboxylic acid (1,4-H_2ndc), to induce Co(II)-core aggregation, and different auxiliary N-donor spacers 1,4-bis(imidazol-1-ylmethyl)-benzene (bix) and 4,4′-bis(triazol-1-ylmethyl)biphenyl (btp) to further tune the structures and properties of the final coordination frameworks. As a result, two high-connected MOFs with Co_5 and Co_8-clusters as nodes have been obtained. Notably, $[Co_5(\mu_3{-}OH)_2(1,4\text{-ndc})_4(bix)_2]_n$ (**1**) shows a quite rare 10-connected self-penetrating **ile** network that can be regarded as the crosslinking of two interpenetrating 6-connected **pcu** nets, while $\{[Co_8(\mu_3{-}OH)_4(1,4\text{-ndc})_6(btp)(H_2O)_6]\cdot H_2O\}_n$ (**2**) has a unique 8-connected self-penetrating ($4^{20}.6^8$) framework. Moreover, their magnetic properties were also investigated and discussed in detail.

EXPERIMENTAL SECTION

Materials and Physical Measurements. All reagents and solvents were commercially available and used as received. Elemental analyses for C, H and N were performed on a Flash 2000 organic elemental analyzer. Thermogravimetric analysis was performed on a Netzsch Model STA 449C microanalyzer heated from 25 °C to 900 °C in nitrogen atmosphere. Infrared spectra (4000−600 cm^{-1}) were recorded on a Fourier transform infrared (FTIR) Nexus spectrophotometer. Powder X-ray diffraction (PXRD) patterns were taken on a Rigaku Ultima IV diffractometer (Cu Kα radiation, λ = 1.5406 Å), with a scan speed of 5°/min and a step size of 0.02° in 2θ. Variable-temperature magnetic measurements were carried out on a Quantum Design SQUID MPMS XL-7 instrument (2−300 K) in the magnetic field of 1 kOe, and the diamagnetic corrections were evaluated using Pascal's constants.

Preparation of Complexes 1 and 2. *$[Co_5(\mu_3{-}OH)_2(1,4\text{-ndc})_4(bix)_2]_n$ (**1**).* A mixture of 1,4-H_2ndc (0.1 mmol, 21.6 mg), bix (0.1 mmol, 23.8 mg), $Co(OCl_4)_2\cdot 6H_2O$ (0.2 mmol, 96.5 mg), NaOH (0.2 mmol, 8.0 mg), and H_2O/EtOH (10 mL, v:v 1:1) was placed in a 25-mL Teflon-lined stainless steel vessel, heated to 140 °C for 3 days, and then cooled to room temperature over 24 h. Purple block crystals of **1** were obtained. Yield: 37.2 mg (56% based on Co(II)). Elemental analysis (%): calcd for ($C_{76}H_{54}Co_5N_8O_{18}$): C 54.92, H 3.26, N 6.74; found: C 55.01, H 3.30, N 6.81. IR (cm^{-1}): 3369m, 1619m, 1585s, 1517m, 1405s, 1356vs, 1107w, 1092w, 822s, 792s, 724s, 686m, 576w, 499w.

*$\{[Co_8(\mu_3{-}OH)_4(1,4\text{-ndc})_6(btp)(H_2O)_6]\cdot H_2O\}_n$ (**2**).* Complex **2** was synthesized in a similar way as that for **1**, except that bix is replaced by btp (0.1 mmol, 31.6 mg). Dark red block crystals were obtained in 46% yield (26.1 mg, based on Co(II)). Elemental analysis (%): calcd for ($C_{90}H_{70}Co_8N_6O_{35}$): C 47.68, H 3.11, N 3.71; found: C 47.71, H 3.13, N 3.76. IR (cm^{-1}): 3439s, 1597s, 1553s, 1458m, 1414s, 1356vs, 1268m, 1209w, 1136w, 1041w, 843s, 799s, 748s, 690m, 563w, 498w.

X-ray Crystallography. Single-crystal X-ray diffraction data for complexes **1** and **2** were collected on a Bruker SMART APEX CCD diffractometer with graphite-monochromated Mo Kα radiation (λ = 0.71073 Å) at room temperature. The structures were solved by direct methods and successive Fourier difference synthesis (SHELXS-97), and refined by the full-matrix least-squares method on F^2 with anisotropic thermal parameters for all non-H atoms (SHELXL-97). H atoms were assigned with isotropic displacement factors and included in the final refinement with geometrical restrains. Further crystallographic data and selected bond parameters for **1** and **2** are shown in Table 1 and Table S1 in the Supporting Information. (See Cambridge Crystallographic Data Centre (CCDC) (Nos. 908060 for **1** and 908061) for **2**.)

Table 1. Crystallographic Data and Structural Refinement Details for 1 and 2

	1	2
formula	$C_{76}H_{54}Co_5N_8O_{18}$	$C_{90}H_{70}Co_8N_6O_{35}$
formula weight	1661.95	2267.00
temperature (K)	296(2)	296(2)
crystal system	monoclinic	monoclinic
space group	$P2_1/c$	$P2_1/c$
a (Å)	15.440(7)	11.4903(9)
b (Å)	15.677(6)	21.7478(3)
c (Å)	16.500(10)	20.8346(5)
β (°)	117.826(5)	91.029(4)
V (Å^3)	3532(3)	5205.5(4)
Z	2	2
D_c (g cm^{-3})	1.563	1.444
μ (mm^{-1})	1.229	1.322
F (000)	1690	2296
θ range (°)	1.91−27.53	2.11−27.53
reflections, collected	37124	55095
independent reflections	8113	11903
R_{int}	0.1486	0.1224
data/restraints/parameters	8113/1/484	11903/0/628
GOOF	1.092	1.089
R_1,[a] wR_2[b] [$I > 2\sigma(I)$]	0.0561, 0.1457	0.0666, 0.1621
R_1, wR_2 (all data)	0.0727, 0.1581	0.0884, 0.1772
$\Delta\rho_{max}$, $\Delta\rho_{min}$ (e Å^{-3})	0.776, −1.017	1.562, −0.755

[a] $R_1 = \sum(|F_0| - |F_c|)/\sum|F_0|$. [b] $wR_2 = [\sum\{w(|F_0|^2 - |F_c|^2)^2\}/\sum[w(|F_0|^2)^2]]^{1/2}$.

RESULTS AND DISCUSSION

Synthetic Chemistry. To explore the role of N-donor bridging ligands on assembly and structural variability of the cluster-based MOFs, a series of solvothermal reactions were attempted. In these solvothermal synthesis, all reactions are the same to mix 1,4-H_2ndc and $Co(ClO_4)_2\cdot 6H_2O$ in H_2O/EtOH (v:v = 1:1), but with various N-donor coligands such as bix, btp, 4,4′-dipyridylsulfide (dps), 1,4-bis-(imidazol)butane (bib), and 1,6-bis(imidazol)hexane (bih). When these co-ligands were applied, respectively, the corresponding different products, for instance, metal cluster-based MOFs **1** and **2**, noncluster-based MOFs $[Co(1,4\text{-ndc})(dps)(H_2O)]_n$ (CCDC No. 908062), $\{[Co(1,4\text{-ndc})(bib)]\cdot 2.5H_2O\}_n$ (CCDC No. 908063), and $[Co(1,4\text{-ndc})(bih)]_n$ (CCDC No. 908064) can be obtained. In this contribution, we will focus on the syntheses, structures, and properties of two Co(II)-cluster based MOFs **1** and **2**.

Previous studies[12] have shown that the formation of metal-clusters $[M_x(\mu_3{-}OH)_y]$ rely on the subtle changes in solvothermal parameters. In this work, it is clear that the bix or btp co-ligand can play a key role in governing the metal clusters $[M_x(\mu_3{-}OH)_y]$ and the final supramolecular structures. So it can be speculated that the longer and flexible N-donor

dx.doi.org/10.1021/ic4007718 | Inorg. Chem. 2013, 52, 8091−8098

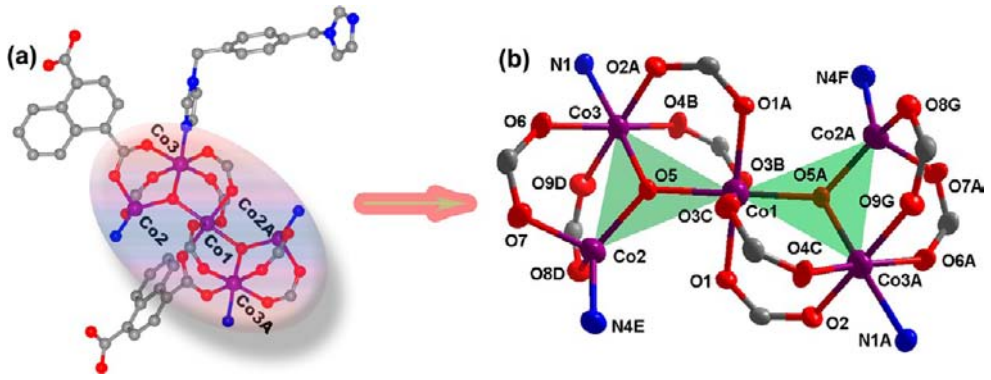

Figure 1. Crystal structure of **1**: (a) coordination environments of Co(II); (b) the pentanuclear $[Co_5(\mu_3{-}OH)_2(COO)_8]$ cluster (symmetry codes: A = $-x+2, -y+1, -z+1$; B = $x, -y+{}^3/_2, z+{}^1/_2$; C = $-x+2, y-{}^1/_2, -z+{}^1/_2$; D = $-x+1, y+{}^1/_2, -z+{}^1/_2$; E = $x, y, z-1$; F = $2-x, 1-y, 2-z$; G = $1+x, {}^1/_2-y, {}^1/_2+z$).

ligand that contains phenyl/biphenyl groups may facilitate the formation of higher-nuclear cluster cores and influence the superstructures of crystal seeds.

Complexes **1** and **2** are air stable, insoluble in common organic solvents, and can retain their crystalline integrity at ambient conditions for a long time. The IR spectra of **1** and **2** show strong absorption bands between 1619 and 1356 cm^{-1} of carboxylates, and no characteristic absorption band of COOH in the range of 1700−1750 cm^{-1} is observed, indicating a complete deprotonation of the ligand. The broad bands at region of 3439−3369 cm^{-1} reveal the presence of water molecules and/or hydroxyl groups.

Crystal Structures. *$[Co_5(\mu_3{-}OH)_2(1,4\text{-ndc})_4(bix)_2]_n$ (**1**).* X-ray structural analysis reveals that compound **1** crystallizes in monoclinic space group $P2_1/c$, the asymmetric unit of which consists of two and a half Co(II) ions with different coordination geometries, two 1,4-ndc^{2-} anions, one bix, and one hydroxyl group. As shown in Figure 1a, Co1, sitting on an inversion center, displays an octahedral sphere surrounded by two $\mu_3{-}OH^-$ (Co1−O5 = 2.079(2) Å) and four carboxylato−O (Co1−O1 = 2.091(2) Å and Co1−O3 = 2.112(2) Å) from different 1,4-ndc^{2-} ligands. Also, Co3 shows an octahedral sphere composed of one $\mu_3{-}OH^-$ (Co3−O5 = 2.072(2) Å), four carboxylato−O (Co3−O2 = 2.121(2) Å and Co3−O6 = 2.139(2) Å) and one nitrogen donor (Co3−N1 = 2.086(2) Å) from bix. While Co2 atom is tetrahedrally bound to one $\mu_3{-}OH^-$ (Co2−O5 = 1.942(2) Å), two carboxylato-O (Co2−O7 = 2.001(2) Å and Co2−O8 = 1.953(2) Å) and one N atom (Co2−N4 = 2.013(2) Å). Although all Co−O bond lengths are comparable to those reported in the literature,[13] the average Co2−O bond (1.965(2) Å) is slightly shorter than that of Co1−O (2.094(2) Å) or Co3−O (2.111(2) Å).

In **1**, two symmetry-related $\mu_3{-}OH^-$ groups (symmetry code: $-x+2, -y+1, -z+1$) connect five Co(II) atoms to form a $[Co_5(\mu_3{-}OH)_2]^{8+}$ cluster subunit, which can be viewed as two $[Co_3(\mu_3{-}OH)]^{4+}$ triangles sharing a common Co1 vertex (Figure 1b). Such triangles are held together by eight carboxylate bridges to constitute the pentanuclear $[Co_5(\mu_3{-}OH)_2(COO)_8]$ cluster (see Figure 1b), which is similar to some known examples.[14] As a result, five Co(II) ions within the pentanuclear clusters are totally coplanar, in which the Co···Co distances are 3.637 Å (Co1···Co2), 3.433 Å (Co1···Co3), and 3.198 Å (Co2···Co3).

Until now, in reported pentanuclear $[Co_5(\mu_3{-}OH)_2]$ cluster-based MOFs,[14] pentanuclear Co_5-clusters usually serve as 6- or 8-connected nodes, which are extended to build intricate 3D frameworks with **pcu**, **mab**, and **scu** topology, respectively. In this case, one type of μ_4-1,4-ndc^{2-} ligand (μ_2-η^1:η^1-C13O6O7 and μ_2-η^1:η^1-C18O8O9) adopt the *syn*−*syn* bridging coordination fashion to link Co2 and Co3, with the distances of 11.091 Å for Co2···Co2 and 11.375 Å for Co3···Co3, affording (4,4) networks with ABAB stacking fashions (see Figures 2a and 2b).

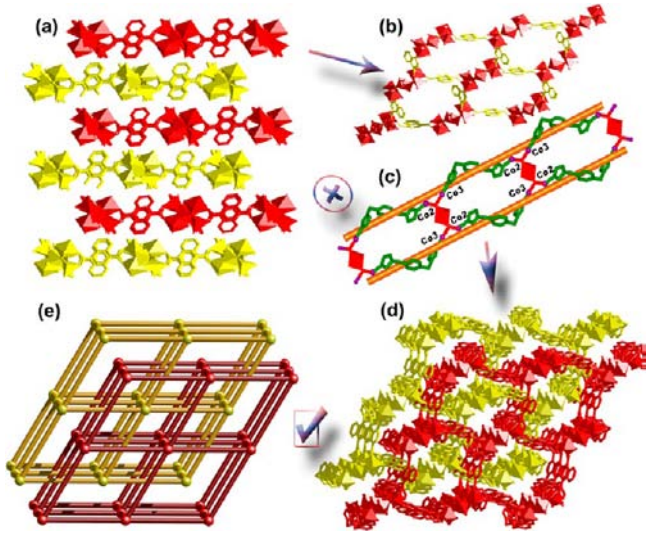

Figure 2. Entangling framework of **1**: (a) the parallel (4,4) network in ABAB fashions; (b) single (4,4) layer; (c) the left- and right-hand helical double chains; (d) 2-fold interpenetrating framework; and (e) 2-fold interpenetrating **pcu** net.

Moreover, the bix ligands adopting *trans*-configuration link Co2 and Co3 ions to form left- and right-hand helical double chains along the *c*-axis (Figure 2c), which cross-link these (4,4) networks into 2-fold interpenetrating 6-connected **pcu** nets (see Figures 2d and 2e). Finally, other μ_4-1,4-ndc^{2-} ligands (μ_2-η^1:η^1-C1O1O2 and μ_2-η^1:η^1-C6O3O4) combine Co1 and Co3 ions of the pentacobalt clusters from neighboring layers in zigzag-chain fashion (Figure 3a, cyan). As a result, two interpenetrating **pcu** nets are linked to generate a self-penetrating framework (Figures 3a and 3b). Topologically, each pentacobalt cluster can be defined as a 10-connected node (see Figures 3c and 3d), and the overall structure of **1** has a uninodal 10-connected self-penetrating **ile**-$(3^6.4^{34}.5^3.6^2)$ (TD10 = 3761) framework analyzed using TOPOS[15] (see Figures 3e and 3g, as well as Table S2 in the Supporting Information).

dx.doi.org/10.1021/ic4007718 | *Inorg. Chem.* 2013, 52, 8091−8098

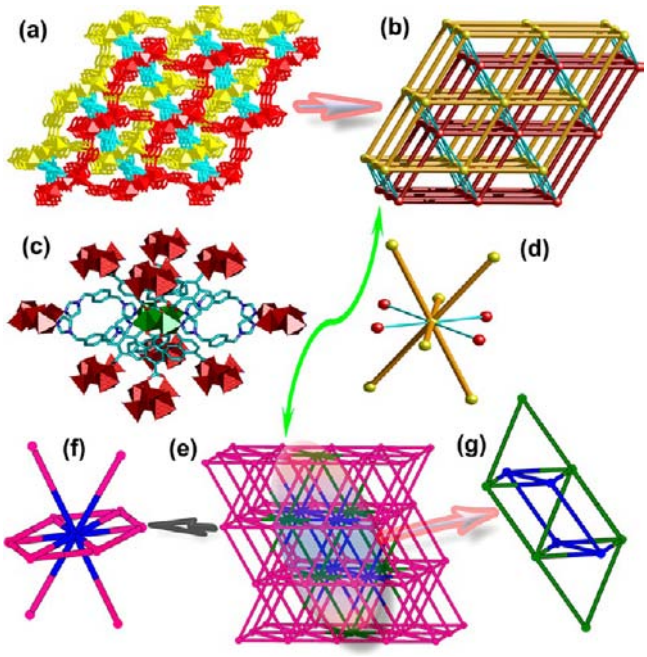

Figure 3. Topological structures of **1**: (a) the 3D framework constructed by 2-fold interpenetrating 6-connected **pcu** nets and zigzag-chains from μ_4-1,4-ndc^{2-}/pentacobalt clusters (cyan); (b) 10-connected self-penetrating net; (c) the linkages of pentacobalt cluster with 10 adjacent cores; (d) 10-connected pentacobalt node; (e) 10-connected self-penetrating **ile**-($3^6.4^{34}.5^3.6^2$) net; (f) the linkages of each center of **hxl**-3^6 net with four different centers in upper and lower layers; (g) perspective views of the ring links between 4-membered shortest rings within the **ile** net.

Notably, this example represents the highest-connected uninodal self-penetrating network based on pentacobalt clusters.

So far, nine different uninodal 10-connected coordination nets have been known: **gpu**-$3^{12}.4^{26}.5^7$ net based on pentanuclear Cd(II) clusters,[11a] ($3^6.4^{31}.5^6.6^2$) net based on [$Ni_2N_4O_6$] dimers,[16a] **bct**-$3^{12}.4^{28}.5^5$ net based on tetranuclear Cd(II) clusters[16b] and trinuclear Co(II) clusters,[16c] **ile**-$3^6.4^{34}.5^3.6^2$ net based on tetranuclear Co(II) clusters[16d] and pentanuclear Zn(II) clusters,[11f] **FeB**-($3^{15}.4^{22}.5^8$) framework based on dinuclear Dy(III),[16e] ($3^{12}.4^{24}.5^9$) net based on Dy(III) ion,[16f] ($3^{10}.4^{25}.5^{10}$) net based on tetranuclear Ca(II) clusters,[16g] ($3^6.4^{23}.5^{13}.6^3$) net based on Cd_{16} clusters[16h] and ($4^{41}.6^4$) net based on trinuclear Cd(II) clusters.[16i] Among them, only four uninodal 10-connected nets have self-penetrating topological configuration, namely, **ile**-$3^6.4^{34}.5^3.6^2$, ($3^6.4^{31}.5^6.6^2$), ($3^6.4^{23}.5^{13}.6^3$), and ($4^{41}.6^4$). In this structure, according to the approach for analysis of high-connected frameworks proposed by Schröder et al.,[17] the 10-fold connectivity of **1** can also be described as being formed from parallel 2D **hxl**-3^6 nets (see Figure 3e), in which each center provides four links to four Co(II) centers in upper and lower layers (Figure 3f). Alternately, this **ile** net can be viewed as the crosslink of two interpenetrating 6-connected **pcu** nets (Figure 3b).

{[$Co_8(\mu_3$–OH)$_4$(1,4-ndc)$_6$(btp)(H_2O)$_6$]·H_2O}$_n$ (**2**). When bix was replaced with the longer btp ligand, an unprecedented 8-connected self-penetrating framework based on octanuclear Co(II) clusters was observed for **2**. The asymmetric unit of **2** contains four independent Co(II) ions, three 1,4-ndc^{2-} anions, one btp, two hydroxyl groups, and three aqua ligands, along with a half lattice water molecule (Figure 4a). Co1, Co2, and Co3 all take the distorted octahedral geometries of [CoO_6] or [CoO_5N]. Co1 and Co2 are coordinated by six O atoms from μ_3–OH$^-$ anions (Co1–O13 = 2.107(2) Å, Co2–O14/O16 = 2.125(2)/2.107(2) Å), three carboxylates of 1,4-ndc^{2-} (Co1–O = 2.059(2)–2.126 (2) Å, Co2–O = 2.067(2)–2.123(2) Å), and two water ligands (Co1–O13 = 2.107(2) Å, Co2–O15 = 2.066(3) Å), respectively. While Co3 is surrounded by five O atoms from one μ_3–OH$^-$ group (Co3–O16 = 2.085(2) Å), three carboxylates (Co3–O = 2.076(2)–2.189(2) Å), one water ligand (Co3–O17 = 2.120(5) Å) and one N atom (Co3–N1 = 2.091(3) Å) from btp ligand. Differently, Co4 is bound to five O atoms from two μ_3–OH$^-$ ions (Co4–O16/O14= 1.992(2)–2.007(2) Å) and three carboxylates (Co4–O = 2.017(2)–2.141(2) Å), resulting in a distorted trigonal bipyramid geometry of [CoO_5]. Four symmetry-related Co1–Co1A, Co2–Co2A, Co3–Co3A, and Co4–Co4A pairs (symmetry code: 1 − *x*, 1 − *y*, 1 − *z*) are ligated by 2 pairs of μ_3–OH$^-$ groups and 12 carboxylate groups to afford a unique centrosymmetric [$Co_8(\mu_3$–OH)$_4$($COO)_{12}$] cluster (see Figure 3b). It can also be viewed as formed by [$Co_3(\mu_2$-O2)(μ_2-O5)(μ_3-O14)(μ_3-O16)] subunits connected through O4 atoms. In the Co_8 cluster, the adjacent Co···Co separations are 3.148 Å for Co1···Co2, 3.260 Å for Co1···Co4, 3.180 Å for Co2···Co3, 3.918 Å for Co2···Co4), 3.607 Å for Co2···Co4A, and 3.531 Å for Co3···Co4A).

In **2**, the 1,4-ndc^{2-} ligands adopt three different types of coordination modes [μ_5-$\eta_{O1}{}^1$:$\eta_{O2}{}^2$:$\eta_{O3}{}^1$:$\eta_{O4}{}^1$ (**A**), μ_4-$\eta_{O5}{}^2$:$\eta_{O6}{}^0$:$\eta_{O7}{}^1$:$\eta_{O8}{}^1$ (**B**) and μ_4-$\eta_{O9}{}^1$:$\eta_{O10}{}^1$:$\eta_{O11}{}^1$:$\eta_{O12}{}^1$ (**C**)] to extend the Co_8 clusters to construct a 6-connected **pcu** network

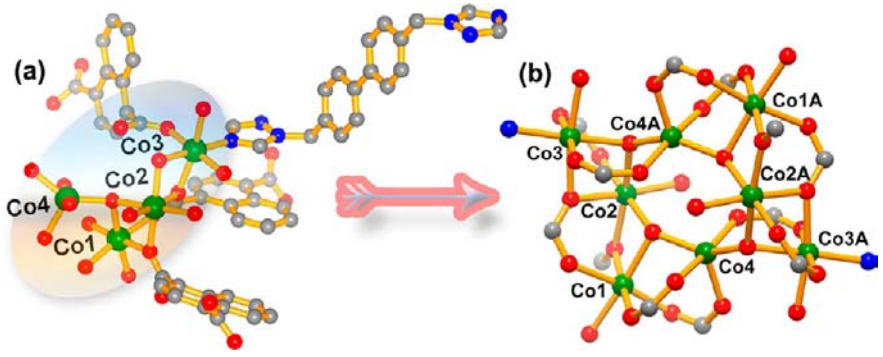

Figure 4. Crystal structure of **2**: (a) coordination environments of Co(II); (b) the octanuclear [$Co_8(\mu_3$–OH)$_4$($COO)_{12}$] cluster (symmetry codes: A = *x* + 1, *y*, *z*).

dx.doi.org/10.1021/ic4007718 | *Inorg. Chem.* 2013, 52, 8091–8098

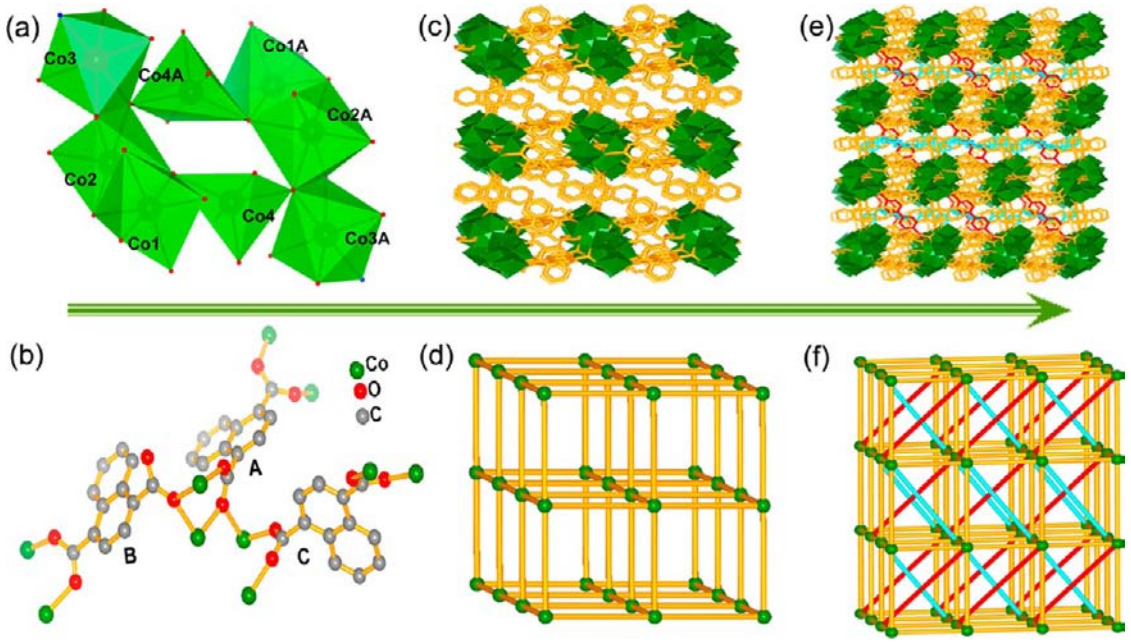

Figure 5. Structural evolution of **2**: (a) the centrosymmetric $[Co_8(\mu_3{-}OH)_4(COO)_{12}]$ cluster; (b) three coordination modes of 1,4-ndc^{2-}, μ_5-$\eta_{O1}{}^1{:}\eta_{O2}{}^2{:}\eta_{O3}{}^1{:}\eta_{O4}$ (**A**), μ_4-$\eta_{O5}{}^2{:}\eta_{O6}{}^0{:}\eta_{O7}{}^1{:}\eta_{O8}{}^1$ (**B**) and μ_4-$\eta_{O9}{}^1{:}\eta_{O10}{}^1{:}\eta_{O11}{}^1{:}\eta_{O12}{}^1$ (**C**); (c) three-dimensional (3D) framework from octacobalt clusters linked by 1,4-ndc^{2-} anions; (d) **pcu** net; (e) the resulting 3D architecture constructed from octacobalt clusters linked by 1,4-ndc^{2-} and *trans*-btp ligands (red and cyan); and (f) 8-connected net.

(see Figures 5a–d). Furthermore, the btp ligands with *trans*-configuration (Figures 5e and 5f: red and cyan) join this **pcu** net to furnish a three-dimensional (3D) 8-connected coordination framework (Figures 5e and 5f), defining a uninodal 8-connected self-penetrating net of ($4^{20}.6^8$) topology (see Figures 6a–6d).

A recent Cambridge Structural Database (CSD) search (version 5.34, Feb. 2013) indicates that there are only several Co_8-cluster cases,[10g] such as the spherelike $[Co_8(\mu{-}O_4)Q_{12}]$ (HQ = 8-hydroxyquinoline),[18a] $[Co_8]$ cage,[18b] cubane-related Co_8 cluster $[Co_8(C_4O_7)_4(H_2O)_{12}]$,[18c] octacobalt phosphonate cage,[18d] cubic nanocage Co_8L_{12} (HL = 4,6-bis(2-pyridyl)-1,3,5-triazin-2-ol),[18e] and other octanuclear Co(II) cluster.[18f] However, only a 3D Co_8-based MOF $[Co8(\mu_3{-}OH)_4(SO_4)_2(dcpbpy)_4{-}(H_2O)_4]{\cdot}12DMF{\cdot}4EtOH{\cdot}24H_2O$[18f] (**MCF-32**, H_2dcpbpy = 2,6-dipcarboxyphenyl-4,4′-bipyridine) has been reported, where 3-connected dcpbpy^{2-} link the 12-connected Co_8-clusters to form a (3,12)-connected porous framework showing gas sorption and spin-glassy magnetic behavior. Thus, complex **2** not only presents a new centrosymmetric octacobalt cluster motif, but also represents the second case of 3D MOFs based on octacobalt clusters.

Recently, 11 uninodal self-penetrating 8-connected nets have been summarized.[19] Significantly, although the net of **2** has the same point symbol with two eight-connected self-penetrating **8T10** or **8T3** net based on trinuclear Cd(II)[19b] or binuclear Ni(II)[19c] SBU, respectively, they exhibit different network topologies with the long vertex symbol of ($4.4.4.4.4_2.4_2.4_2.4_2.4_2.4_2.4_2.4_2.4_2.4_2.4_2.4_2.4_2.4_3.4_3.4_3.4_3.6_6.6_{20}.6_{20}.6_{21}.6_{21}.6_{21}.6_{21}.6_{26}$) for **2** (TD10 = 3599, see Table S3 in the Supporting Information), ($4.4.4.4.4.4.4.4.4.4.4.4.4.4.4.4.4.4.4.4.4.4.6_2.6_2.6_{14}.6_{14}.6_{14}.6_{14}.7_{40}.7_{40}$) for **8T10** net (TD10 = 5637),[19b] and ($4.4.4.4.4_2.4_2.4_2.4_2.4_2.4_2.4_2.4_2.4_2.4_2.4_2.4_2.4_2.4_3.4_3.4_3.4_3.6_6.6_6.6_6.6_6.6_{10}.6_{10}.6_{10}.6_{10}$) for **8T3** net (TD10 = 3091),[19c] respectively. On the other hand, the main difference between **2**, **8T10**, and **8T3** net is that only the shortest six-membered

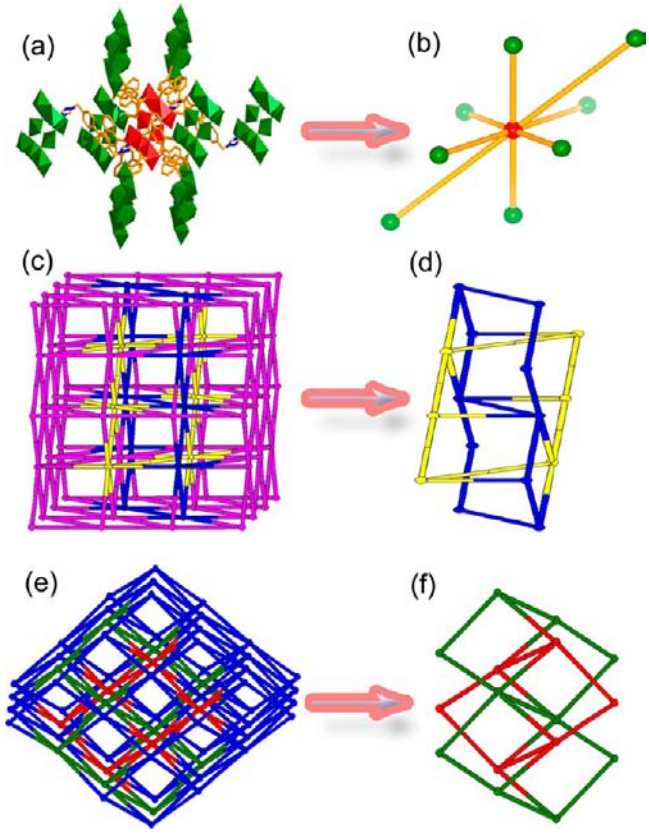

Figure 6. Topological structure of **2**: (a) the linkage of the Co_8 cluster with eight adjacent cores; (b) 8-connected octacobalt node; (c) 8-connected self-penetrating ($4^{20}.6^8$) net; (d) the ring links between 6-membered shortest rings; (e) 8-connected self-penetrating **8T3** net; and (f) the ring links between 6-membered shortest rings of **8T3** net.

dx.doi.org/10.1021/ic4007718 | *Inorg. Chem.* 2013, 52, 8091–8098

rings are interlocked in **2** and **8T3** nets (see Figures 6a and 6e), while the shortest four-membered and six-membered rings are interlocked in an **8T10** net.[19a] A careful analysis using TOPOS[15] indicates that the nonequivalent 6-membered shortest rings of **2** (6^8, $6_6.6_{20}.6_{20}.6_{21}.6_{21}.6_{21}.6_{21}.6_{26}$) and **8T3** ($6^8$, $6_6.6_6.6_6.6_6.6_{10}.6_{10}.6_{10}.6_{10}$) are catenated and connected in different ways (28 in **2** and 81 in **8T3**; see Table S4 in the Supporting Information), and as a representative Hopf link (see Figures 6d and 6f). Thus, **2** is a new, three-periodic 8-connected self-penetrating network and also represents the highest-connected uninodal self-penetrating network based on octacobalt clusters.

Structural Comparison. As discussed above, complexes **1** and **2** are composed of centrosymmetric $[Co_5(\mu_3{-}OH)_2(COO)_8]$ and $[Co_8(\mu_3{-}OH)_4(COO)_{12}]$ clusters as SBUs, respectively, in which the Co(II) centers adopt a variety of coordination spheres including $[CoO_6]$, $[CoO_5N]$, and $[CoO_3N]$ for **1** and $[CoO_6]$, $[CoO_5N]$, and $[CoO_5]$ for **2**. Also, the 1,4-ndc^{2-} anions take different bridging modes (μ_4- for **1**, μ_4- and μ_5- for **2**), which incorporate the *trans*-configuration bix and btp spacers, respectively, to extend the Co5 or Co8 clusters in distinct ways, resulting in rare, highly connected, self-penetrating networks. In fact, although complexes **1** and **2** were obtained under similar solvothermal conditions, the presence of different N-donor ligands is responsible for their significant structural discrepancy. In this sense, the auxiliary N-donor ligands play an important role in governing the coordination clusters and the final supramolecular structures in such assembled systems.

PXRD and TG Results. In order to check the phase purity of bulk materials for **1** and **2**, powder X-ray diffraction (PXRD) patterns were recorded at room temperature (see Figure S1 in the Supporting Information). The peak positions of experimental and simulated PXRD patterns are in good agreement, which confirm their phase purity. The difference in intensity of some diffraction peaks may be attributed to the preferred orientation of the crystalline samples.

Thermogravimetric (TG) experiments were performed on single-crystal samples of **1** and **2** in the temperature range of 30−900 °C (Figure S2 in the Supporting Information). Complex **1** is thermally stable up to 295 °C, beyond which the framework begins to collapse and the final residual weight is likely attributed to CoO (calc. 22.54% and exp. 23.30%). Complex **2** first loses the lattice and coordinated water in 70−191 °C region (calc. 5.56% and exp. 5.96%), and the residue remains largely unchanged until heating to 310 °C, whereupon expulsion of the organic components occurs. Also, the final mass remnant of 27.33% likely represents the deposition of CoO solid (26.44% calcd) at 523 °C.

Magnetic Properties. The temperature-dependent magnetic susceptibilities were measured on polycrystalline samples of **1** and **2** at 1000 Oe in the range of 1.8−300 K. For **1**, as shown in Figure 7, the value of $\chi_M T$ at 300 K is 12.01 cm^3 mol^{-1} K, which is larger than the calculated spin-only value (9.375 cm^3 mol^{-1} K) for five Co(II) (S = $^3/_2$) ions, indicating the orbital contribution arising from the high-spin octahedral Co(II). Upon cooling, $\chi_M T$ decreases monotonously to achieve a minimum value of 0.95 cm^3 mol^{-1} K at 2 K, suggesting an appreciable antiferromagnetic exchange between the Co(II) ions connected through two μ_3−O and O−C−O bridges. The Co1−O5−Co2, Co1−O5−Co3, and Co2−O5−Co3 angles are 129.46(11)°, 111.59(10)°, and 105.59(11)°, respectively. These large Co−O−Co angles, as well as the *syn*−*syn* bridging

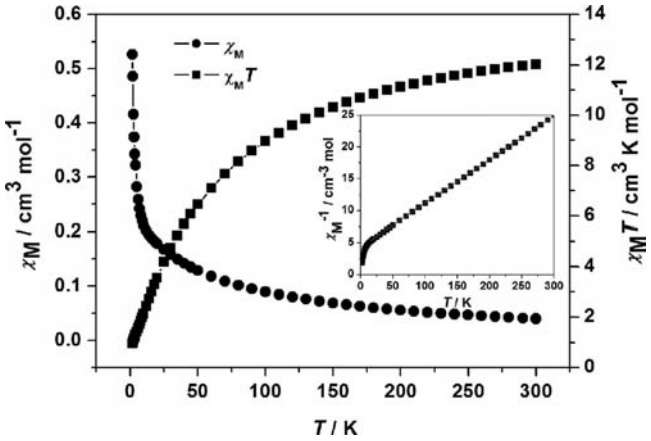

Figure 7. Temperature dependence of $\chi_M T$ and χ_M versus T of **1**. Inset: temperature dependence of χ_M^{-1}; the solid line represents the best fit of the Curie−Weiss law $\chi_M = C/(T - \theta)$.

mode of the carboxylate group, are generally indications of antiferromagnetic interactions.[20] Above 15 K, the temperature dependence of $1/\chi_M$ obeys the Curie−Weiss law with C = 14.55 cm^3 K mol^{-1} and θ = −62.1 K (see Figure 7, insert), revealing dominant antiferromagnetic interactions between the Co(II) ions and the presence of spin−orbit couplings.

The field dependence of magnetization of **1** at 2 K is shown in Figure S3 in the Supporting Information. The magnetization at 2 K and an applied filed of 50 kOe is 5.73 Nβ per Co_5 unit. This value is higher than the value of one Co(II), and lower than that for three Co(II) ions in an octahedral environment with S = $^1/_2$ and g = 4.1−5.0. In the structure description, Co_5 contains two Co_3 triangular units. In these antiferromagnetic trinuclear Co_3 units, the spin frustration is one of the important magnetic phenomena, and usually causes the variety, degeneracy, and mediated spin value of the ground spin state. The $\chi_M T$ value, which is 0.95 cm^3 mol^{-1} K at 2 K lower than that for isolated Co(II) may be due to the frustration effect. However, the intercluster interactions cannot be excluded. In addition, the ac magnetic susceptibility data for **1** were recorded with switching frequencies of 1, 10, 100, 1100 Hz (see Figure S4 in the Supporting Information), and nonfrequency dependency has been detected down to 1.8 K. It demonstrates that compound **1** is not a single molecule magnet (SMM).

The $\chi_M T$ and χ_M versus T plots of **2** are shown in Figure 8. The $\chi_M T$ value at 300 K is 20.77 cm^3 K mol^{-1}, which is much higher than the spin-only value of 15.0 cm^3 K mol^{-1} expected for eight S = $^3/_2$ spins with g = 2, because of the significant spin−orbital coupling of Co(II) centers[21] and the ferromagnetic exchanges between Co(II) ions. Upon cooling, $\chi_M T$ first decreases smoothly to reach a minimum value of 12.10 cm^3 mol^{-1} K at 25 K, then increases to a maximum of 13.81 cm^3 mol^{-1} K at 7.0 K, and finally decreases smoothly to 12.84 cm^3 mol^{-1} K at 1.8 K. This observation of a shallow minimum is as expected for a ferrimagnetic-like behavior, and the decrease of $\chi_M T$ below 7 K may be attributed to interchain antiferromagnetic interactions and/or zero-field splitting of the anisotropic high-spin Co(II) ions.[22] Above 50 K, the temperature dependence of $1/\chi_M$ obeys the Curie−Weiss law, with C = 24.16 cm^3 K mol^{-1} and θ = −50.2 K, indicating dominant antiferromagnetic interactions between the Co(II) ions and the presence of spin−orbit coupling.[23]

The field dependence of magnetization of **2** at 2 K is shown in Figure 9. For high-spin octahedral Co(II) center, the overall

dx.doi.org/10.1021/ic4007718 | Inorg. Chem. 2013, 52, 8091−8098

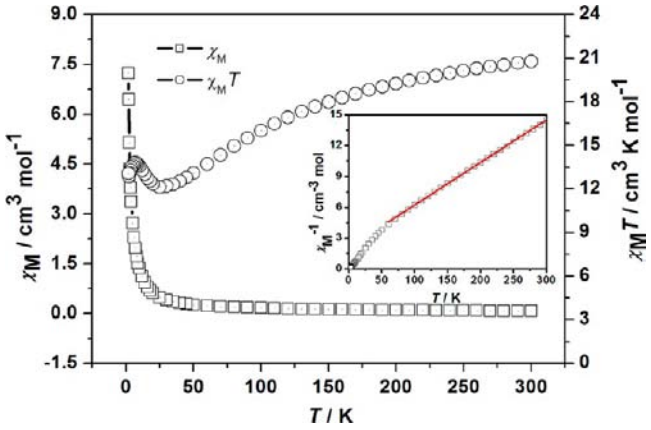

Figure 8. Temperature dependence of $\chi_M T$ and χ_M versus T for **2**. Inset: temperature dependence of χ_M^{-1}; the solid line represents the best fit of the Curie–Weiss law $\chi_M = C/(T - \theta)$.

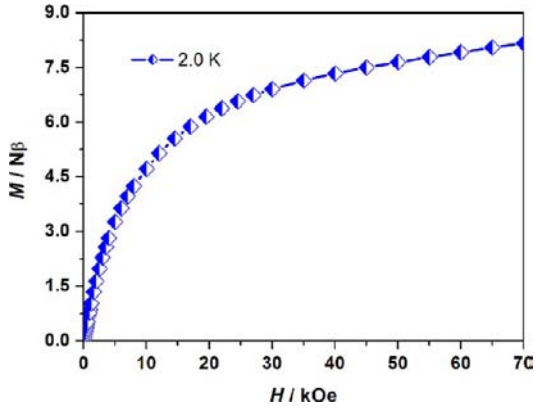

Figure 9. Field dependence of magnetization for **2**.

effect of low-symmetry crystal-field components and spin–orbit coupling split the $^4T_{1g}$ ground state into six Kramers doublets and result in a doublet ground state. In low-temperature region (T < 30 K), only the two lowest Kramers doublets are significantly populated and Co(II) systems may be described as having an effective spin of $^1/_2$ with large anisotropy. As described in the structure, complex **2** contains Co_8 cluster formed by $[Co_3(\mu_2\text{–}O)_2(\mu_3\text{–}O)_2]$ units interconnected through O4 atoms. Within the Co_3O_4 units, the magnetic interactions between Co1···Co2, Co2···Co3, and their symmetry equivalents are transmitted via two μ_2–O and two μ_3–O pathways, with Co1–O5–Co2, Co1–O14–Co2, Co2–O2–Co3, and Co2–O16–Co3 angles of 95.57(9)°, 94.91(8)°, 95.22(9)°, and 98.68(9)°, respectively, which generally leads to ferromagnetic interactions between the Co(II) ions.[24] The exchange pathways between Co1···Co4, Co2···Co4, Co3···Co4, and their symmetry equivalents involve μ_3–O and *syn–syn* carboxylate bridges, in which Co1–O14–Co4, Co2–O14–Co4, Co2–O16–Co4A, and Co3–O16–Co4A angles are 103.36(9)°, 143.02(11)°, 123.18(11)°, and 119.99(10)°. These values are in the range of antiferromagnetic interactions.[21] Magnetization at 2 K and an applied filed of 70 kOe is 8.16 Nβ per Co_8 unit. This value is close to the expected saturation value for four octahedral Co(II) ions with S = $^1/_2$ and g = 4.1–5.0, which is consistent with a ferrimagnetic-like state arising from the coexistence of both ferromagnetic and antiferromagnetic exchange interactions within the Co_8 unit. Besides, the ac magnetic susceptibility data for **2** were recorded with switching frequencies of 1, 10, 100, and 1100 Hz (see Figure S5 in the Supporting Information), and nonfrequency dependency has been detected in the temperature range of 1.8–16 K. It demonstrates that compound **2** is not a SMM, although Co_8 shows a ferrimagnetic spin ground state.

CONCLUSIONS

In summary, two high-connected Co(II) coordination frameworks with different cluster units have been prepared under solvothermal conditions, using Co(II) perchlorate and 1,4-naphthalene dicarboxylic acid with the introduction of rationally selected N-donor ancillary ligands in a H_2O/EtOH system. For **1**, pentanuclear $[Co_5(\mu_3\text{–}OH)_2(COO)_8]$ clusters are interlinked into a rare three-dimensional (3D) 10-connected self-penetrating **ile** net that can be considered as the crosslinking of two interpenetrating 6-connected **pcu** networks. For **2**, the octanuclear $[Co_8(\mu_3\text{–}OH)_4(COO)_{12}]$ clusters are extended to form a 3D 8-connected self-penetrating $(4^{20}.6^8)$ framework, which is the highest-connected uninodal self-penetrating motif based on octacobalt clusters. That is, the overall coordination frameworks can be well-modulated by the N-donor coligands. Magnetic studies reveal that **1** shows an antiferromagnetic exchange between the Co(II) ions, while dominant antiferromagnetic interactions (in 300–50 K) and ferrimagnetic-like behaviors (at lower temperatures) are observed in **2**. These results further enrich our knowledge of structural topologies for coordination networks, and they also confirm the promising potential of auxiliary ligand-directed assembled strategy for the design of new cluster-based MOFs with unique structures and properties.

ASSOCIATED CONTENT

Supporting Information

X-ray crystallographic information for **1** and **2** in CIF format, tables of selected bond parameters and topological linking modes of short-rings, and PXRD and TG plots for **1** and **2**. This material is available free of charge via the Internet at http://pubs.acs.org.

AUTHOR INFORMATION

Corresponding Author

*Tel./Fax: +86 717 6397516 (D.-S.L.), +86 29 88302604 (B.L.), +86 22 23766556 (M.D.). E-mail address: lidongsheng1@126.com (D.-S.L.), liubin@nwu.edu.cn (B.L.), dumiao@public.tpt.tj.cn (M.D.).

Notes

The authors declare no competing financial interest.

ACKNOWLEDGMENTS

This work was financially supported by NSF of China (Nos. 21073106, 21031002, 21101126, and 21201109) and NSF of Hubei Province of China (No. 2011CDA118). M.D. also thanks the support from Tianjin Normal University.

REFERENCES

(1) (a) Hoskins, B. F.; Robson, R. *J. Am. Chem. Soc.* **1989**, *111*, 5962. (b) Hoskins, B. F.; Robson, R. *J. Am. Chem. Soc.* **1990**, *112*, 1546.

(2) (a) *Chem. Rev.* **2012**, *112* (2), 673–1268 (Special thematic issue on Metal-Organic Frameworks). (b) *Chem. Soc. Rev.* **2011**, *40* (2), 453–1152 (Special Thematic Issue on Hybrid Materials,). (c) *Chem. Soc. Rev.* **2009**, *38* (5), 1201–1508 (Themed issue on Metal-Organic Frameworks).

(3) (a) *Metal-Organic Frameworks. Applications from Catalysis to Gas Storage*; Farrusseng, D., Ed.; Wiley−VCH Verlag & Co. KGaA: Weinheim, Germany, 2011. (b) *Metal-Organic Frameworks. Design and Application*; MacGillivray, L., Ed.; Wiley−VCH Verlag & Co. KGaA: Weinheim, Germany, 2011.
(4) (a) Batten, S. R.; Neville, S. M.; Turner, D. R. *Coordination Polymers Design, Analysis and Application*; The Royal Society of Chemistry: London, 2009; pp 273−372. (b) Yaghi, O. M.; O'Keeffe, M.; Ockwig, N. W.; Chae, H. K.; Eddaoudi, M.; Kim, J. *Nature* **2003**, *423*, 705. (c) Tranchemontagne, D. J.; Mendoza-Cortes, J. L.; O'Keeffe, M.; Yaghi, O. M. *Chem. Soc. Rev.* **2009**, *38*, 1257. (d) Perry, J. J., IV; Perman, J. A.; Zaworotko, M. J. *Chem. Soc. Rev.* **2009**, *38*, 1400. (e) Zeng, Y. F.; Hu, X.; Liu, F. C.; Bu, X. H. *Chem. Soc. Rev.* **2009**, *38*, 469.
(5) (a) Li, J. R.; Timmons, D. J.; Zhou, H. C. *J. Am. Chem. Soc.* **2009**, *131*, 6368. (b) Zhou, Y. L.; Zeng, M. H.; Wei, L. Q.; Li, B. W.; Kurmoo, M. *Chem. Mater.* **2010**, *22*, 4295. (c) Leng, J. D.; Liu, J. L.; Tong, M. L. *Chem. Commun.* **2012**, *48*, 5286. (d) Escuer, A.; Vlahopoulou, G.; Mautner, F. A. *Inorg. Chem.* **2011**, *50*, 2717.
(6) Kostakis, G. E.; Powell, A. K. *Coord. Chem. Rev.* **2010**, *259*, 2686.
(7) (a) Zheng, S. T.; Bu, J. J.; Wu, T.; Chou, C.; Feng, P.; Bu, X. *Angew. Chem., Int. Ed.* **2011**, *50*, 8858. (b) Lan, Y. Q.; Jiang, H. L.; Li, S. L.; Xu, Q. *Inorg. Chem.* **2009**, *51*, 7484.
(8) (a) Férey, G.; Mellot-Draznieks, C.; Serre, C.; Millange, F.; Dutour, J.; Surblé, S.; Margiolaki, I. *Science* **2005**, *309*, 2040. (b) Jia, J. H.; Lin, X.; Wilson, C.; Blake, A. J.; Champness, N. R.; Hubberstey, P.; Walker, G.; Cussen, E. J.; Schröder, M. *Chem. Commun.* **2007**, 840. (c) Zheng, Y. Z.; Tong, M. L.; Xue, W.; Zhang, W. X.; Chen, X.-M.; Grandjean, F.; Long, G. J. *Angew. Chem., Int. Ed.* **2007**, *46*, 607. (d) Mondal, K. C.; Kostakis, G. E.; Lan, Y.; Anson, C. E.; Powell, A. K. *Inorg. Chem.* **2009**, *48*, 9205. (e) Zhang, Y. B.; Zhou, H.-L.; Lin, R. B.; Zhang, C.; Lin, J. B.; Zhang, J.-P.; Chen, X. M. *Nat. Commun.* **2012**, *3*, 642.
(9) (a) Kurmoo, M. *Chem. Soc. Rev.* **2009**, *38*, 1353. (b) Murrie, M. *Chem. Soc. Rev.* **2010**, *39*, 1986. (c) Boca, R. *Coord. Chem. Rev.* **2004**, *248*, 757. (d) Weng, D.-F.; Wang, Z.-M.; Gao, S. *Chem. Soc. Rev.* **2011**, *40*, 3157. (e) Dechambenoit, P.; Long, J. R. *Chem. Soc. Rev.* **2011**, *40*, 3249. (f) Forster, P. M.; Stock, N.; Cheetham, A. K. *Angew. Chem., Int. Ed.* **2005**, *44*, 7608.
(10) (a) Wang, X. L.; Qin, C.; Lan, Y. Q.; Shao, K. Z.; Su, Z. M.; Wang, E. B. *Chem. Commun.* **2009**, 410. (b) Morris, J. J.; Noll, B. C.; Henderson, K. W. *Chem. Commun.* **2007**, 5191. (c) Li, D.; Wu, T.; Zhou, X. P.; Zhou, R.; Huang, X. C. *Angew. Chem., Int. Ed.* **2005**, *44*, 4175. (d) Cairns, A. J.; Perman, J. A.; Wojtas, L.; Kravtsov, V. C.; Alkordi, M. H.; Eddaoudi, M.; Zaworotko, M. J. *J. Am. Chem. Soc.* **2008**, *130*, 1560. (e) Sarma, D.; Mahata, P.; Nataraian, S.; Panissod, P.; Gogez, G.; Drillon, M. *Inorg. Chem.* **2012**, *51*, 4495. (f) He, K. H.; Song, W. C.; Li, Y. W.; Chen, Y. Q.; Bu, X. H. *Cryst. Growth Des.* **2012**, *12*, 1064. (g) Kostakis, G. E.; Perlepes, S. P.; Blatov, V. A.; Proserpio, D. M. *Coord. Chem. Rev.* **2012**, *256*, 1246.
(11) (a) Li, D. S.; Fu, F.; Zhao, J.; Wu, Y. P.; Du, M.; Zou, K.; Dong, W. W.; Wang, Y. Y. *Dalton Trans.* **2010**, *39*, 11522. (b) Ma, L. F.; Wang, L. Y.; Du, M.; Batten, S. R. *Inorg. Chem.* **2010**, *49*, 365.
(12) (a) Chen, Q.; Xue, W.; Lin, J. B.; Lin, R. B.; Zeng, M. H.; Chen, X. M. *Dalton Trans.* **2012**, *41*, 4199. (b) Chen, Q.; Xue, W.; Wang, B. Y.; Zeng, M. H.; Chen, X. M. *CrystEngComm* **2012**, *14*, 2009. (c) Chen, Q.; Lin, J. B.; Xue, W.; Lin, R. B.; Zeng, M. H.; Chen, X. M. *Inorg. Chem.* **2011**, *50*, 2321.
(13) (a) Lin, Z.; Wragg, D. S.; Warren, J. E.; Morris, R. E. *J. Am. Chem. Soc.* **2007**, *129*, 10334. (b) Jia, H. P.; Li, W.; Ju, Z. F; Zhang, J. *Dalton Trans.* **2007**, 3699.
(14) (a) Li, B.; Zhou, X.; Zhou, Q.; Li, G.; Hua, J.; Bi, Y.; Li, Y.; Shi, Z.; Feng, S. *CrystEngComm* **2011**, *13*, 4592. (b) Duan, X.; Cheng, X.; Lin, J.; Zang, S.; Li, Y.; Zhu, C.; Meng, Q. *CrystEngComm* **2008**, *10*, 706. (c) Hu, S.; Liu, J. L.; Meng, Z. S.; Zheng, Y. Z.; Lan, Y.; Powell, A. K.; Tong, M. L. *Dalton Trans.* **2011**, *40*, 27.
(15) Blatov, V. A. *TOPOS, A Multipurpose Crystallochemical Analysis with the Program Package*; Samara State University, Samara, Russian Federation, 2004.
(16) (a) Luis, R. F. D.; Mesa, L.; Urtiaga, M. K.; Lezama, L.; Arriortua, M. I.; Rojo, T. *New J. Chem.* **2008**, *32*, 1582. (b) Song, W. C.; Pan, Q.; Song, P. C.; Zhao, Q.; Zeng, Y. F.; Hu, T. L.; Bu, X. H. *Chem. Commun.* **2010**, *46*, 4890. (c) Su, Z.; Song, Y.; Bai, Z. S.; Fan, J.; Liu, G. X.; Sun, W. Y. *CrystEngComm* **2010**, *12*, 4339. (d) Yang, J.; Li, B.; Ma, J. F.; Liu, Y. Y.; Zhang, J. P. *Chem. Commun.* **2010**, *46*, 8383. (e) Karmakar, A.; Goldberg, I. *CrystEngComm* **2011**, *13*, 339. (f) Liang, L.; Peng, G.; Ma, L.; Sun, L.; Deng, H.; Li, H.; Li, W. *Cryst. Growth Des.* **2012**, *12*, 1151. (g) Gu, Z. G.; Liu, Y. T.; Hong, X. J.; Zhan, Q. G.; Zheng, Z. P.; Zheng, S. R.; Li, W. S.; Hu, S. J.; Cai, Y. P. *Cryst. Growth Des.* **2012**, *12*, 2178. (h) Zhai, Q. G.; Niu, J. P.; Li, S. N.; Jiang, Y. C.; Hu, M. C.; Batten, S. R. *CrystEngComm* **2011**, *13*, 4508. (i) Hu, J. S.; Shang, Y. J.; Yao, X. Q.; Qin, L.; Li, Y. Z.; Guo, Z. J.; Zheng, H. G.; Xue, Z. L. *Cryst. Growth Des.* **2010**, *10*, 4135.
(17) Hill, R. J.; Long, D. L.; Champness, N. R.; Hubberstey, P.; Schröder, M. *Acc. Chem. Res.* **2005**, *38*, 337.
(18) (a) Cheng, X. N.; Xue, W.; Lin, J. B.; Chen, X. M. *Chem. Commun.* **2010**, *46*, 246. (b) Langley, S.; Helliwell, M.; Sessoli, R.; Teat, S. J.; Winpenny, R. E. P. *Inorg. Chem.* **2008**, *47*, 497. (c) Abrahams, B. F.; Hudson, T. A.; Robson, R. *J. Am. Chem.. Soc.* **2004**, *126*, 8634. (d) Langley, S. J.; Helliwell, M.; Sessoli, R.; Rosa, P.; Wernsdorfer, W.; Winpenny, R. E. P. *Chem. Commun.* **2005**, 5029. (e) Cao, M. L.; Hao, H. G.; Zhang, W. X.; Ye, B. H. *Inorg. Chem.* **2008**, *47*, 8126. (f) Hou, L.; Zhang, W. X.; Zhang, J. P.; Xue, W.; Zhang, Y. B.; Chen, X. M. *Chem. Commun.* **2010**, *46*, 6311.
(19) (a) Ke, X. J.; Li, D. S.; Du, M. *Inorg. Chem. Commun.* **2011**, *14*, 788. (b) Wang, X. L.; Qin, C.; Wang, E. B.; Su, Z. M. *Chem.—Eur. J.* **2006**, *12*, 2680. (c) Yang, G. S.; Lan, Y. Q.; Zang, H. Y.; Shao, K. Z.; Wang, X. L.; Su, Z. M.; Jiang, C. J. *CrystEngComm* **2009**, *11*, 274.
(20) (a) Ghoshal, D.; Mostafa, G.; Maji, T. K.; Zangrando, E.; Lu, T. H.; Ribas, J.; Chaudhuri, N. R. *New J. Chem.* **2004**, *28*, 1204. (b) Jia, H. P.; Li, W.; Ju, Z. F.; Zhang, J. *Eur. J. Inorg. Chem.* **2006**, 4264. (c) Jia, H. P.; Li, W.; Ju, Z. F.; Zhang, J. *Inorg. Chem. Commun.* **2007**, *10*, 265.
(21) (a) Konar, S.; Mukherjee, P. S.; Drew, M. G. B.; Ribas, J.; Chaudhuri, N. R. *Inorg. Chem.* **2003**, *42*, 2545. (b) Humphrey, S. M.; Wood, P. T. *J. Am. Chem. Soc.* **2004**, *126*, 13236. (c) Calvo-Pérez, V.; Ostrovsky, S.; Vega, A.; Pelikan, J.; Spodine, E.; Haase, W. *Inorg. Chem.* **2006**, *45*, 644. (d) Duan, Z. M.; Zhang, Y.; Zhang, B.; Zhu, D. B. *Inorg. Chem.* **2008**, *47*, 9152. (e) Cao, D. K.; Li, Y. Z.; Zheng, L. M. *Inorg. Chem.* **2007**, *46*, 7571. (f) Wang, Z. M.; Zhang, B.; Inoue, K.; Fujiwara, H.; Otsuka, T.; Kobayashi, H.; Kurmoo, M. *Inorg. Chem.* **2007**, *46*, 437.
(22) (a) Tong, M. L.; Kitagawa, S.; Chang, H. C.; Ohba, M. *Chem. Commun.* **2004**, 418. (b) Berry, J. F.; Cotton, F. A.; Liu, C. Y.; Lu, T. B.; Murillo, C. A.; Tsukerblat, B. S.; Villagían, D.; Wang, X. P. *J. Am. Chem. Soc.* **2005**, *127*, 4895.
(23) Li, X. J.; Wang, X. Y.; Gao, S.; Cao, R. *Inorg. Chem.* **2006**, *45*, 1508.
(24) (a) Chiang, R. K.; Huang, C. C.; Wur, C. S. *Inorg. Chem.* **2001**, *40*, 3237. (b) Du, M.; Guo, Y. M.; Bu, X. H.; Ribas, J. *Eur. J. Inorg. Chem.* **2004**, 3228.